Eco. Env. & Cons. 30 (4) : 2024; pp. (1554-1561)
Copyright@ EM International
ISSN 0971–765X

DOI No.: http://doi.org/10.53550/EEC.2024.v30i04.014

Landscape Ecological Risk Assessment in the Southwestern Fringe of Guwahati City, India

Rakesh Kumar Sarmah*[1] and Santanu Sarma[2]

Department of Geology, Cotton University, Guwahati 781 001, Assam, India

(Received 18 May, 2024; Accepted 12 July, 2024)

ABSTRACT

Rapid urbanization targets in developing countries often underestimate the ecological balance between nature and humanity. Urban fringe or peri-urban landscapes need critical attention due to their increased vulnerability as areas for potential investments and rural-urban jurisdiction dichotomy. Through this study, an attempt has been made to assess the spatiotemporal landscape ecological risk associated with the south western fringe areas of Guwahati city using remote sensing and GIS technology. The Landsat satellite imagery from 1991 and 2011 is utilized to analyse the land use land cover (LULC) dynamics using random tree classifier technique. For accuracy enhancement, Normalized Difference Vegetation Index (NDVI) and the Normalized Difference Building index (NDBI) are incorporated. Standard formulae are used to determine the landscape ecological risk in a grid approach, and Bayesian kriging interpolation is adopted for the representation of the results. During this period the built-up area increased from 34.95 km^2 to 74.72 km^2. The increase in built-up areas is more prominent towards the north, adjacent to the Guwahati airport. 17.90% of cropland and 12.60% of sparse vegetation mainly contributed to this increment. The cropland area decreased from 121.87 km^2 to 104.11 km^2. The change in sparse vegetation is more compared to dense vegetation. The sparse vegetation patches are converted mainly into built-up, dense vegetation, and cropland. Sandbars, swamp/waterlogging, and waterbodies show a decrease in this period. The landscape ecological risk results show the concentration of high-risk areas in the central valley portion of the study area for 1991 covering 27.26%, which gradually shifted towards the south in 2011 with 15.11% area coverage. The sub-high-risk area also shows a significant increase in area coverage from 22.38% to 33.33%. The medium and sub-low-risk areas show a small increment from 21.56% to 23.92% and 18.41% to 19.13% respectively. The low-risk areas show a decrement from 10.39% to 8.52% during this time frame. The study will provide a sustainable framework integrating ecological values in urban planning and policy-making.

Key words : *Landscape ecological Risk, Urban fringe, LULC, Spatial planning, GIS*

Introduction

Urban footprints expand with the cost of agricultural lands, wildlife habitat, and alteration of regional hydrology often causing complete landscape transformation (Gunerlap *et al.*, 2020). In developing countries, government policies mainly focus on rapid urbanization targeting a large population percentage to bring under urban arena in a short period resulting in massive population movement, changing traditional social structure with large infrastructure investment in comparison to the leisurely pace in developed countries in a more sustainable way (Henderson, 2014). Rapid urbanization causes ‘ecological stress’ that needs critical attention during policy decisions (Li and Cao, 2019). Urbanization

([1]Research Scholar, [2]Professor)

causes loss of natural vegetation, depletion of open spaces, decline in spatial extent, and connectivity of wetlands and wildlife habitat (Saleh and Rawashdeh, 2007). The ecological risk assessment in the context of urbanization involves addressing the adverse impacts of human activities on the ecosystem and its components (Zhang *et al.*, 2020). There is a global concern for landscape sustainability through governance, e.g. the European Landscape Convention 2020 to promote conservation through legislation (Cheng *et al*., 2023). However, in developing countries, local governments face a contradictory dilemma to maintaining the integrity of the ecosystem on one hand, and promoting regional economic development through rapid urbanization on the other, resulting in socio-ecological instability (Ding *et al*., 2019). Development plans for fringe areas are often under-valued as they come under the jurisdiction of local governments beyond urban authorities. Urban growth is a continuous spatial-temporal process and a function of three driving forces-a *physical, socio-economic, and environmental*, complex interaction that leads to changes in land use patterns (Weerakoon, 2017). Land use dynamics can be best visualized and analyzed using remote sensing and GIS technology. Multi-temporal satellite data is of priority among researchers in analyzing urban dynamics (Ramachandra *et al*., 2014, Boori *et al*., 2014, Ojima and Hogan, 2009). Ecological landscape signifies land-use types with significant ecological values contributing to water conservation, wildlife protection, and balancing different aspects of microclimate. Urbanization as an anthropogenic driver results in habitat fragmentation reducing biomass and creating fragile isolated fragments (Cheng *et al.*, 2022).

The current study aims at a quantitative spatiotemporal assessment of the dynamics of the periurban landscapes of Guwahati City, India with associated risks to the fragile ecological land covers using Remote Sensing and GIS technology.

Materials and Methods

Study area: The southwestern fringe of Guwahati city is an ecologically sensitive zone with a mosaic of wetlands, reserve forests, fertile agricultural lands, and rivers undergoing a rural-urban transition at a rapid pace. For this study, the combined area of two fringe administrative blocks, Rani and Chayani Barduar are considered with an area coverage of 422.40 sq. km with 129 villages. The area is marked towards the north by the east-west flowing mighty river Brahmaputra, towards the west by river Kulshi, a major tributary channel of river Brahmaputra, towards the south and southeast the elevated hills of Shillong plateau, and the northeast by the Guwahati City. The flood plains and alluvial plains of river Brahmaputra, piedmont zones, and denudational hills of Shillong plateau are major physiographic features within the study area. Granitic gneisses are the dominant rock units within the

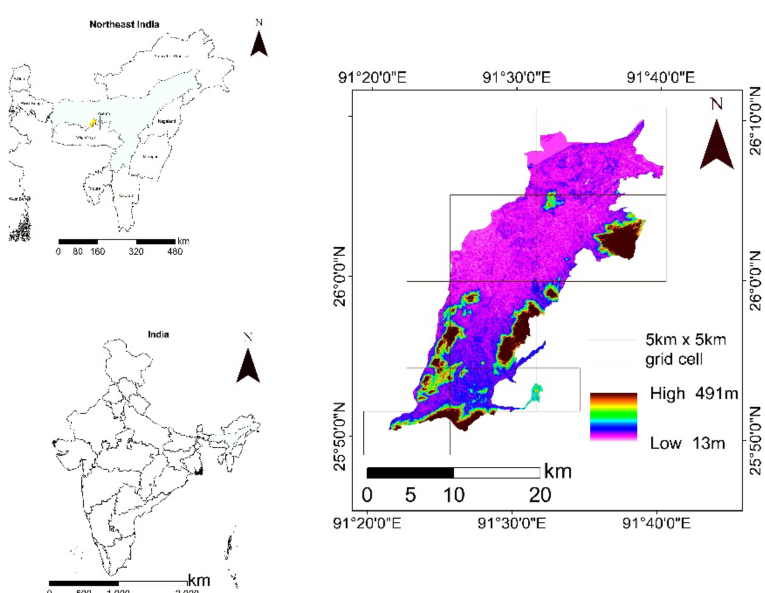

Fig. 1. Study area map

elevated hills. The hills are covered by dense vegetation with deciduous and evergreen species and are demarcated as reserve forests. There are six reserve forests within the study area namely Barduar, Dakhin Rani, Jarasal, Kawasing, Maliya, and Mataikhar, with rich floral and faunal presence. The part of the Deepor Beel Lake, a Ramsar site towards the northeast, and Chandubi Lake towards the south play significant ecological significance in the area. The area witnesses a tropical monsoon type of climate with rainfall during the summer between June to September with an average temperature range of 35 ºC to 9 ºC. Urbanization is prominent towards the north adjacent to the Lokpriya Gopinath Bordoloi International Airport, Guwahati. The proximity to the airport and the city makes this area attractive avenue for investors due to low property and service tax. Already agricultural lands have been converted into small and large-scale industries; apartment and apartment complexes are being developed due to the lack of open space within the main city; business complexes, hotels, etc. are mushrooming.

Preparation of Land Use/ Land Cover (LULC)

The spatiotemporal analysis of land use/land cover of the study area is carried out using the Landsat imageries for 1991, and 2011 available at the Earth Explorer platform of USGS (https://earthexplorer.usgs.gov/).

The ERDAS Imagine software is used for necessary processing such as layer stacking, geometric correction, and masking of the study area. The 1:50,000 scale 1972 Survey of India topographic maps are used as a reference layer. LULC maps are prepared using the train random tree classifier tool of ArcGIS 10.7 considering sufficient training samples from each LULC class. The Normalized Difference Vegetation Index (NDVI) and the Normalized Difference Building Index (NDBI) are also calculated to enhance classification accuracy. Using Google Earth Imagery and on-field ground control points the classification accuracy (kappa coefficient) has been enhanced above 85% for both years. The 1991 Landsat 5 contains the Thematic Mapper (TM) sensor, which possesses multi-spectral scanning capabilities in 7 spectral bands. Band 4 (Near Infrared) and band 3 (Red) are utilized for the determination of the Normalized Difference Vegetation Index (NDVI).

$$NDVI = \frac{NIR - R}{NIR + R}$$

The NDVI value ranges between -1 and +1, the value is negative for water bodies, and for land use classes like rocks, sand, and concrete surfaces, the value is close to zero. The value is positive for vegetative features like crops, shrubs, grasses, and forests (Huang *et al*., 2021). Another important index for the estimation of various land use classes is the normalized difference building index (NDBI) calculated using Band 5 (SWIR 1) and Band 4 (NIR) of Landsat 5.

$$NDBI = \frac{SWIR\,1 - NIR}{SWIR\,1 + NIR}$$

The value of NDBI ranges between –1 and +1 where positive values of NDBI represent urban land use and negative values of NDBI represent non-urban land use features (Zheng *et al*., 2021). For 2011 Landsat 7 imagery, the sensor onboard is Enhanced Thematic Mapper Plus (ETM+) having 8 spectral bands. Band 4 (NIR) and Band 3 (Red) are used for NDVI calculation and Band 5 (SWIR 1), and Band 4 (NIR) are used for NDBI calculation. Using standard literature, different thresholds are applied for NDVI and NDBI for both years, analyzing differences in tones for different features (Badlani *et al.,* 2017; Miranda *et al.,* 2018) a total of five LULC types are classified as follows: Dense Vegetation, Sparse Vegetation, Built-up, Cropland, Swamp/ Waterlogging, Water body and Sandbar (Figure 2). The dense vegetation mainly includes forest and dense fluvial vegetation adjacent to the wetlands, the sparse vegetation includes scrubs, rural household plantation, and grasslands, the Built-up areas are mainly concrete man-made features, the croplands are mainly paddy fields adjacent to the settlements, swamp/ waterlogging areas include marshy features within

Table 1. The details of Landsat Imageries used for the study are as follows

Satellite	Raw	Path	Date of Acquisition	Spatial Resolution
Landsat 5 TM	42	137	26-11-1991	30m
Landsat 7 ETM+	42	137	05-06-2011	30m

the flood plains of river Brahmaputra, waterbodies are mainly wetlands, rivers and ponds, the sandbars within river Brahmaputra and its tributaries.

Evaluation of Ecological Risk Index (ERI)

The landscape ecological risk index of the study area is calculated using the landscape disturbance index and fragility index. The landscape disturbance index indicates the degree of influence of human disturbance on a certain landscape type (Lin and Wang, 2023). The landscape fragility index represents the resistance ability of a landscape to such disturbances (Li *et al.*, 2017). The research communities commonly use the following formulas to evaluate ERI (Yu *et al.*, 2019; Gao and Song, 2022; Wang *et al.*, 2021).

Referring to the earlier literature and considering the spatial heterogeneity, the study area is divided into 32 grid cells (represents risk subarea sample units) with 5 km × 5 km dimension. ERI value for each grid cell is calculated, normalized, and assigned to the centroid of each grid. The values for the centroids are interpolated for the entire study area using the empirical Bayesian kriging in ArcGIS 10.7 software. The final ERI values are classified into five classes using the natural breaks method: low risk, sub-low risk, medium risk, sub-high risk, and high-risk areas (Figure 3a, 3c).

Table 2. Formulas commonly used for landscape ecological risk index evaluation

Index	Formula	Description
Fragmentation Index (F_i): represents landscape transition from a single continuous entity to complex discontinuous patches	$Fi = \frac{N_i}{A_i}$	Where, n_i is the number of patches of landscape *i*, A_i is the area of landscape
Splitting Index (S_i): degree of separation between different patches within a landscape	$S_i = \frac{A}{2A_i} \sqrt{\frac{n_i}{A}}$	Where, A is the total area
Landscape Dominance Index (D_i): the importance of certain patches in the entire landscape	$D_i = \frac{(Q_i+M_i)}{4} + \frac{L_i}{2}$ $Q_i = \frac{n_i}{N}, L_i = \frac{A_i}{A}, M_i = \frac{B_i}{B}$	Where, *N* is the total patch number, B_i is the number of samples for landscape i, *B* is the total number of samples
Landscape Disturbance Index (LDI_i) : degree of influence of human disturbance on a certain landscape type	$LDIi = aF_i + bS_i + cD_i$	Where, a, b, c are the weights of the landscape metrics such that a + b + c = 1, using standard literature a = 0.5, b = 0.3, and c = 0.2
Landscape Fragility Index (LFI) indicates resistance ability or vulnerability	For this study, based on literature review the vulnerabilities of different landscape types are arranged from low to high as follows: built-up, dense vegetation, sandbar, sparse vegetation, swamp/ waterlogging, waterbody and cropland. The values are then normalized to get the final	Landscape Fragility Index LFI_i for the landscape
Ecological Risk Index (ERI) : indicates degree of comprehensive ecological losses in a sample plot and can adequately reflect the possible changes in ecological risks attributed to landscape pattern changes.	$ERI = \sum_{i}^{j} \frac{A_{ki}}{A_k} \sqrt{LDI_i \quad LFI_i}$	Where, A_{ki} is the area of landcape i in sample k and A_k is the area of sample

Spatial Autocorrelation Analysis

Spatial Autocorrelation depicts patterns in the distribution of geographic variables based on their location and attribute information (Sharma *et al.*, 2018). The global and local Moran's I spatial autocorrelation techniques are selected to evaluate the spatial distribution of the ERI values whether the pattern expressed is clustered, dispersed, or random using the following formulas (Abdulhafedh, 2017):

The global Moran's I can be calculated for n observations on a variable x at locations (i,j)

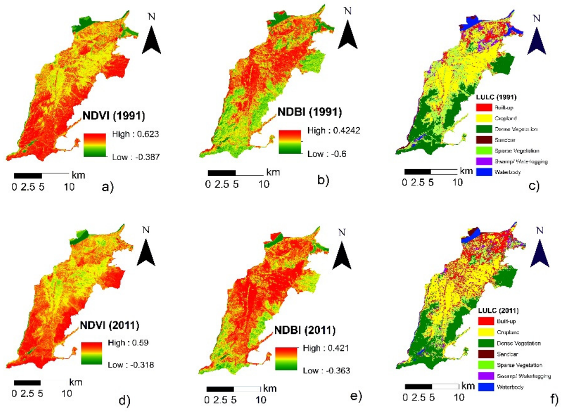

Fig. 2. a) NDVI, b) NDBI, c) LULC map for 1991 and d) NDVI, e) NDBI, f) LULC map for 2011

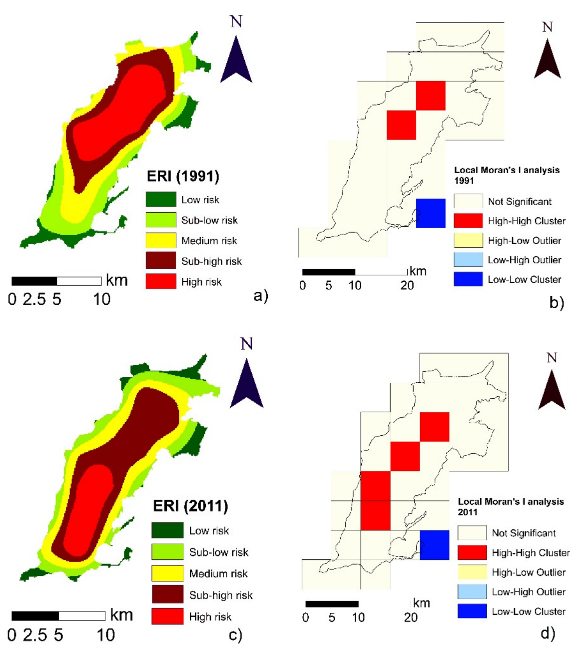

Fig. 3. a) ERI map for 1991, b) Local Moran's I map for 1991 and c) ERI map for 2011, d) Local Moran's I map for 2011

$$I = \frac{n}{S_0} \frac{\sum_i^n \sum_j^n w_{ij} \quad (x_i - \bar{x}) \quad (x_j - \bar{x})}{\sum_i^n (x_i - \bar{x})^2}$$

Where, $\bar{x}$ = the mean of the variable x, x_i = the value of the variable x at location i, x_j = the value of the variable at location j, W_{ij} = the elements of the weight matrix, n = number of observations, S_0 = Sum of the elements of the weight matrix = $\Sigma_i^n \Sigma_j^n w_{ij}$

The Global Moran's I value ranges from -1 (perfect dispersion) to +1 (perfect clustering), where 0 indicates perfect randomness.

The formula for local Moran's I :

$$I_i = \frac{x_i - \bar{x}}{S_i^2} \sum_{j=1}^{n} w_{ij} (x_j - \bar{x})$$

Where, $S_i^2 = \frac{\sum_{j=1}^{n} (x_j - \bar{x})^2}{n-1} - \bar{x}^2$

$$E(I) = \frac{-1}{n-1}$$

Moran's I value greater than indicates positive autocorrelation and smaller indicates negative spatial autocorrelation. The result gives five classes: high-high, low-low (clustered pattern), low-high, high-low (outlier pattern), and not-significant (Shariati *et al.*, 2020) (Figure 3b, 3d).

Results and Discussion

Changes in Land Use/ Land Cover

Between 1991 and 2011 significant changes occurred in LULC patterns and statistics within the study area. In 1991, the built-up area was 34.95 km^2, which increased to 74.72 km^2 in 2011, indicating a gradual increase in urbanization.

The cropland area and sparse vegetation are mainly converted to the built-up category. During this period 17.90 % of cropland and 12.60% of sparse vegetation areas of 1991 are converted into built-up. These conversions took place more toward the northern side adjacent to the airport. Patches of swamp areas are also converted to built-up. Another important observation is the conversion of croplands to waterlogging/ swamp areas. 3.72% of cropland areas are converted into swamp/waterlogging category. This is due to the fragmentation of the croplands due to urban impact creating isolated patches of waterlogged areas. The dense vegetation in forest areas is almost intact, however small fragmental changes are noticed in the fringe areas of these reserve forests through their conversion to built-up and cropland caused by anthropogenic activities. There is a 10.01% conversion of sparse vegetation to dense vegetation category. The sandbars are used for the cultivation of seasonal vegetables due to their high fertility. 31.01% of the sanbars are converted into croplands. Sparse riverine grasses, and new swamp/waterlogging patches due to changes in river courses also bring changes to the sandbar. There is not much significant change in the waterbody category.

Changes in Ecological Risk Index (ERI)

The Bayesian Kriging results in 1991 depict the concentration of the high-risk areas within the central valley portion of the study area. The fragmented mixed landuse types adjacent to the airport with croplands as dominant landuse intermingled with spare vegetation as rural settlements enhances the ERI value. This accounts for 27.26% of the total study area (115.23 km^2). The sub-high-risk area encircling the high-risk area accounts for 22.38% (94.59 km^2). Towards the north, it is more of an intermixing of heterogeneous classes and towards the south, fragmentation of the dense vegetation/ forest fringes by rural settlements (household plantations as sparse vegetation) and croplands.

The medium (21.56%, 91.1 km^2) and sub-low categories (18.41%, 77.79 km^2) are relatively less fragmented land use types in comparison to the high and sub-high categories and can be seen in both north and south. The low-risk category (10.39%, 43.92 km^2) areas are found mainly towards the south and east within the reserve forests due to less anthropogenic impacts. The 2011 results show a prominent shift of high-risk zones (15.11%, 63.88 km^2) towards the south due to increase in anthropogenic activities in the fringe areas of forest patches, the conversion of sparse vegetation covers to dense vegetation within this time frame, and agricultural practices in dotted patches. The sub-high category shows an increment during this period with 33.33% coverage of the total area including the central and northern portions. The medium category risk area shows a slight increase with coverage of 23.92% of the total area. The sub-low and low categories cover 19.13% and 8.52% respectively and their spatial distribution is almost like the 1991 analysis (Table 4).

Spatial Autocorrelation results of Ecological Risk Index (ERI)

The value of Global Moran's I ERI analysis is found to be 0.41 for 1991 (where the z-score is 3.17 and the p-value is 0.0015) and 0.27 for 2011 (where, the z-

Table 3. The LULC change matrix between 1991 and 2011

2011 1991	Built-up	Cropland	Dense Vegetation	Sandbar	Sparse Vegetation	Swamp/ Waterlogging	Waterbody	Grand Total
Built-up	34.95							34.95
Cropland	21.81	88.97		0.01	6.43	4.53	0.12	121.87
Dense Vegetation	0.99	0.98	99.40		11.87			113.25
Sandbar		1.33		0.94	0.58	0.59	0.84	4.29
Sparse Vegetation	14.25	9.03	11.32	0.01	74.56	3.92		113.09
Swamp/ Waterlogging	2.72	3.39		0.34	8.01	4.77	1.08	20.33
Waterbody		0.40	0.76	2.36	1.89	1.46	7.74	14.62
Grand Total	74.72	104.11	111.48	3.67	103.35	15.28	9.78	422.40

Table 4. Ecological Risk Index for 1991 and 2011

ERI classes	Area coverage (km^2), 1991	Percentage (%), 1991	Area coverage (km^2), 2011	Percentage (%), 2011
low risk	43.92	10.39	36	8.52
sub-low risk	77.79	18.41	80.87	19.13
medium risk	91.10	21.56	101.13	23.92
sub-high risk	94.59	22.38	140.90	33.33
high-risk	115.23	27.26	63.88	15.11

score is 2.15 and the p-value is 0.03). The values indicate significant spatial autocorrelation for both years. The local Moran's I result for 1991 show significant high-high clusters in the central valley portion of the study area and low-low cluster towards the extreme south. The result for 2011 shows the presence of high-high clusters both in the central part and towards the south, and low-low cluster at a similar location as in 1991.

Conclusion

During the study period, the built-up area increased from 8.27% to 17.68 % portraying significant urban expansion. There is a slight decrease in cropland area from 28.85% to 24.64%. Towards the north, fragmentation of the cropland due to built-up activity results in isolated patches of waterlogging. The study area lies within the Brahmaputra floodplain and is dominated by swamps and marshes which play a significant role in flood management and urban hydrology. There is a decrease in swamp area from 4.81% to 3.61%. The dense vegetation within the study area is mainly reserve forests, balancing urbanization and the natural environment. This category has little change except for a minor fragmental change in the fringe areas. The spatial distribution of the ecological risk index shows the shifting of high-risk areas from the central valley portion towards the south. This is due to increased anthropogenic activities with fragmented landuse practices such as agricultural activities in dotted patches. The sub-high-risk area increases significantly during this period, from 22.38% to 33.33%. Together with the high-risk areas, it accounts for 48.44% of the study area. The Global Moran's I result shows a positive z-score and significant p-value indicating the distribution of high and/or low values in the dataset is more spatially clustered. The Local Moran's I analysis shows the concentration of high-high and low-low clusters in perfect agreement with the ERI distribution. Landscape ecological risk evaluation has limitations due to errors inherent in land cover classification, scale factor, and complexity of landscape as a mosaic of discrete patches. The study will contribute to sustainable urban policy-making considering ecological aspects.

Acknowledgement

The authors wish to express their gratitude to various governmental and non-governmental organizations for providing valuable data.

Conflict of interest

The authors declare that no funds, grants, or other support were received during the preparation of this manuscript. There is no conflict of interest.

References

Abdulhafedh, A. 2017. A novel hybrid method for measuring the spatial autocorrelation of vehicular crashes: combining Moran's Index and Getis-Ord * Gi statistic. *Open Journal of Civil Engineering*. 7:208-221.

Badlani, B., Patel, A.N., Patel, K. and Kalubarme, M.H. 2017. Urban Growth Monitoring using Remote Sensing and Geo-Informatics: Case Study of Gandhinagar, Gujarat State (India). *International Journal of Geosciences*.8: 563-576.

Boori, M.S., Choudhary, K., Kupriyanov, A. and Kovelskiy, V. 2016. Satellite data for Singapore, Manila and Kuala Lumpur city growth analysis. *Data in Brief*. 7:1576-1583.

Cheng, P., Qin, Y., Zhu, S. and Kong, X. 2022. Ecological disturbance of rural settlement expansion: evidence from Nantong, eastern China. *Land*. 11(1741): 1-16.

Cheng, X., Zhang, Y., Yang, G., Nie, W., Wang, Y., Wang, J. and Xu, B. 2023. Landscape ecological risk assessment and influencing factor analysis of basins in suburban areas of large cities – A case study of the Fuchunjiang River Basin, China. *Frontiers in Ecology and Evolution*. 11(1184273): 1-18.

Ding, X., Zhou, C., Zhong, W., and Tang, P. 2019. Addressing uncertainty of environmental governance in environmentally sensitive areas in developing countries: A precise-strike and spatial-targeting adaptive governance framework. *Sustainability*. 11(4510): 1-34.

Gao, H. and Song, W. 2022. Assessing the landscape ecological risks of land-use change. *International Journal of Environmental Research and Public Health*. 19(13945): 1-25.

Güneralp, B., Reba, M., Hales B.U., Wentz, E.A. and Seto, K.C. 2020. Trends in urban land expansion, density, and land transitions from 1970 to 2010: a global synthesis. *Environmental Research Letters*. 15(4): 1-13.

Henderson, J. V. 2010. Cities and Development. *Journal of Regional Science*. 50(1): 515–540.

Huang, S., Tang, L., Hupy, J.P., Wang, Y. and Shao, G. 2021. A commentary review on the use of normalized difference vegetation index (NDVI) in the era of popular remote sensing. *Journal of Forestry Research*. 32(1):1-6.

Li, J., Pu, R., Gong, H., Luo, X., Ye, M. and Feng, B. 2017. Evolution characteristics of landscape ecological risk patterns in coastal zones in Zhejiang Province, China. *Sustainability.* 9(584): 1-18.

Lin, X. and Wang, Z. 2023. Landscape ecological risk assessment and its driving factors of multi-mountainous city. *Ecological Indicators*. 146(109823): 1-15.

Li, P., and Cao, H. 2019. Comprehensive assessment on the ecological stress of rapid land urbanization per proportion, intensity, and location. *Ecosystem Health and Sustainability*. 5(1): 242–255.

Miranda, C.D.S., Filho, A.C.P. and Pott, A. 2018. Changes in vegetation cover of the Pantanal wetland detected by Vegetation Index: a strategy for conservation. *Biota Neotropica*. 18(1): 1-6.

Ojima, R. and Hogan, D.J. 2009. Mobility, Urban Sprawl and Environmental Risks in Brazilian Urban Agglomerations: Challenges for Urban Sustainability, p. 281-316. In: de Sherbiniin, A., Rahman, A., Barbieri, A., Fotso, J.C., Zhu, Y. (Eds) Urban Population-Environment Dynamics in the Developing World: Case Studies and Lessons Learned, Committee for International Cooperation in National Research in Demography (CICRED), Paris, France.

Ramachandra, T. V., Bharath, A. H. and Sowmyashree, M. V. 2015. Monitoring urbanization and its implications in a mega city from space: spatiotemporal patterns and its indicators. *Journal of Environmental Management*. 148: 67–81.

Saleh, B. and Rawashdeh, S.A. 2007. Study of Urban Expansion in Jordanian Cities Using GIS and Remote Sensing. *International Journal of Applied Science and Engineering*. 5 (1): 41-52.

Shariati, M., Mesgari, T., Kasraee, M. and Jahangiri-rad, M. 2020. Spatiotemporal analysis and hotspots detection of COVID-19 using geographic information system (March and April, 2020). *Journal of Environmental Health Science and Engineering*. 18(2): 1499-1507.

Sharma, P., Chandel, V.B.S. and Kahlon, S. 2018. Spatial autocorrelation technique for landslide hot-spot analysis in the upper Ravi River catchment, Chamba, Himachal Pradesh. *The Indian Geographical Journal*. 93(1): 1-9.

Wang, H., Liu, X., Zhao, C., Chang, Y., Liu, Y. and Zang, F. 2021. Spatial-temporal pattern analysis of landscape ecological risk assessment based on land use/ land cover change in Baishuijiang National nature reserve in Gansu Province, China. *Ecological Indicators.* 124(107454): 1-11.

Weerakoon, P. 2017. GIS integrated spatio-temporal urban growth modelling: Colombo urban fringe, Sri Lanka. *Journal of Geographic Information System*. 9: 372-389.

Yu, T., Bao, A., Xu, W., Guo, H., Jiang, L., Zheng, G., Yuan, Y. and Nzabarinda, V. 2019. Exploring variability in landscape ecological risk and quantifying its driving factors in the Amu Darya delta. *International Journal of Environmental Research and Public Health*. 17(79): 1-21.

Zhang, W., Chang, W.J., Zhu, Z.C. and Hui, Z. 2020. Land scape ecological risk assessment of Chinese coastal cities based on land use change. Applied Geography. 117(102174).

Zheng, Y., Tang, L. and Wang, H. 2021. An improved approach for monitoring urban built-up areas by combining NPP-VIIRS nighttime light, NDVI, NDWI, and NDBI. *Journal of Cleaner Production*. 328(129488): 1-13.